PCGF6 licenses DNA methylation at H3K9me3-marked CpG islands to preserve developmental potential in mouse embryonic stem cells.

Mitsuhiro Endoh[1,2], Tamie Endoh[2], Hitoshi Niwa[2], Haruhiko Koseki[3] and Satoru Miyagi[1]
[1] Department of Biochemistry, Faculty of Medicine, Shimane University
[2] Institute of Molecular Embryology and Genetics (IMEG), Kumamoto University
[3]RIKEN Center for Integrative Medical Sciences (IMS)
mendoh@med.shimane-u.ac.jp

A central question in biology is how cells "remember" the right gene-expression program while they transition from one cellular state to another. In early development, pluripotent stem cells can generate many cell types, but this ability changes stepwise as cells move toward differentiation (Ref#1). These transitions require stable control of gene activity, supported by epigenetic mechanisms such as chromatin modifications and DNA methylation.

We previously showed that the Polycomb complex PCGF6–PRC1.6 is essential for maintaining pluripotent stem-cell integrity by repressing germ cell–related genes (Ref#2). Here, using mouse embryonic stem cells (mESCs), we uncover an unexpected role of PCGF6 in coordinating Polycomb-mediated repression with two classical "silencing" features of chromatin: H3K9me3 (a histone mark) and DNA methylation at CpG islands (CGIs).

We propose a two-step model for DNA methylation at specific CGIs during pluripotency transitions: (1) Priming: the PRC1.6 subunit MGA recruits the ATF7IP-SETDB1 machinery via its FAM motif, creating local H3K9me3. This step prepares the chromatin environment but has limited immediate impact on transcription. (2) Licensing: PCGF6 reinforces transcriptional repression via H2AK119ub1 and antagonizes the activity of pluripotency factors DPPA2/4, thereby creating a chromatin environment permissive for DNA methylation at target CGIs.

Our functional analysis reveals that loss of either the Priming (MGA FAM mutation) or the Licensing (*Pcgf6* deficiency) module leads to a significant reduction in DNA methylation levels at target CGIs. Notably, embryonic lethality caused by *Pcgf6* loss is rescued by deleting *Dppa2*, supporting a functional antagonism between PCGF6-dependent licensing and DPPA2/4-mediated protection. Together, our findings identify PCGF6 as a molecular bridge that integrates multiple epigenetic layers to stabilize cellular identity during developmental transitions.

References:
1) M. Endoh and H.Niwa. Stepwise pluripotency transitions in mouse stem cells. EMBO Rep. e55010. 2022
2) M. Endoh et al., PCGF6-PRC1 suppresses premature differentiation of mouse embryonic stem cells by regulating germ cell-related genes. Elife. e21064. 2017

The cell lineage and the developmental mechanism of the cholinergic neurons in the brain of the *Ciona* larva

Kouhei Oonuma[1] and Takehiro G Kusakabe[2]
[1]Faculty of Life and Environmental Sciences, Shimane University
[2]Department of Biology, Konan University
koonuma@life.shimane-u.ac.jp

Ascidians are invertebrate chordates that are the closest relatives of vertebrates, and the nervous system development of ascidians closely resembles that of vertebrates. In addition, the larval brain (brain vesicle) of ascidians is composed of only a few hundred cells. Therefore, ascidians serve as excellent model organism for elucidating brain developmental mechanisms shared with vertebrates at the single-cell resolution. However, in the commonly used ascidian *Ciona robusta* (Fig. 1), a standard embryonic manipulation (removal of the chorion) severely disrupts the structure of the brain vesicle. As a result, the development of individual neurons within the brain vesicle remains poorly understood. To overcome this methodological limitation, we established a microinjection technique for introducing exogenous genes without removing the chorion. Using this approach, we aim to elucidate the cell lineages and developmental mechanisms of brain vesicle neurons.

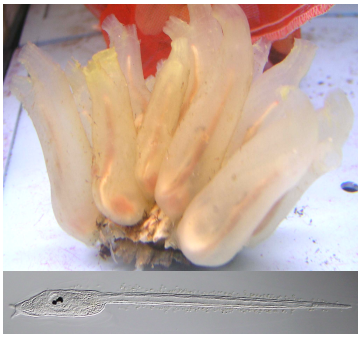

Fig. 1. Adult (upper) and larval (lower) stages of the ascidian *Ciona robusta*.

Cholinergic neurons are one of the major classes of excitatory neurons in the vertebrate central nervous system. In the *Ciona* larva, cholinergic neurons are located in the brain vesicle and the motor ganglion. For the cholinergic neurons in the motor ganglion, their cell lineages, key genes involved in their development, and their roles in the control of larval swimming behavior have been reported. In contrast, the development and functional roles of the cholinergic neurons in the brain vesicle remain largely unknown.

In this study, we investigated the cell lineages and developmental mechanisms of cholinergic neurons in the ascidian brain vesicle without removing the chorion. Lineage tracing using the fluorescent dye revealed that these neurons originate from a single left blastomere at the 8-cell stage. Because the transcription factor FoxB is expressed on the left side of the brain vesicle, we examined whether FoxB regulates cholinergic neuron development. *FoxB* overexpression increased the number of cells expressing the cholinergic marker gene *VAChT*. We also examined the role of Nodal signaling which is essential for regulating left-right asymmetry during animal development. Inhibition of Nodal signaling abolished *VAChT* expression in the brain vesicle, whereas *Nodal* overexpression increased the *VAChT*-positive cells. Notably, simultaneous overexpression of *FoxB* and *Nodal* resulted in a stronger effect than either manipulation alone. These results suggest that coordinated regulation by Nodal signaling and FoxB is essential for the development of the cholinergic neurons in the brain vesicle of *Ciona* larvae.

Functional analysis of fatty acid acyl-CoA reductases in *Euglena gracilis*

[1]Hiroaki Morita, [1'2]Takahiro Ishikawa
[1]*Graduate School of Natural Science and Technology, Shimane University, Japan;*[2] *Institute of Agricultural and Life Sciences, Academic Assembly, Shimane University, Japan*

n25m826@matsu.shimane-u.ac.jp
ishikawa@life.shimane-u.ac.jp

Euglena gracilis, a unicellular phytoflagellated protist, adapts to hypoxic environments through a unique metabolic pathway known as wax ester fermentation. Under low-oxygen conditions, *E. gracilis* degrades its storage polysaccharide paramylon into glucose, which is metabolized via glycolysis to generate ATP. The resulting pyruvate is converted into acetyl-CoA, which is further utilized for fatty acid biosynthesis through the reverse β-oxidation pathway. A portion of the resulting fatty acyl-CoAs is reduced to fatty alcohols, and these are subsequently esterified with fatty acids in the microsomes—primarily forming myristyl myristate (C28). In our laboratory, we previously identified wax ester synthase/diacylglycerol acyltransferase (WSD), the enzyme responsible for the final step of wax ester synthesis [1]. However, the upstream enzyme fatty acid acyl-CoA reductase (FAR), which is responsible for fatty alcohol production, remains poorly understood. Three putative FAR orthologs (FAR1–FAR3) have been predicted in the *E. gracilis* RNA-Seq data [2], but their specific roles in wax ester synthesis have not been elucidated. In this study, we aimed to clarify the functional roles of each FAR isoform.

Bioinformatic analyses revealed that all three FARs possess an NADPH-binding domain characteristic of FAR enzymes. Predicted subcellular localizations suggest that FAR1 localizes to peroxisomes, FAR2 to mitochondria, and FAR3 to the cytosol. To assess their involvement in wax ester synthesis, we performed gene knockdown (KD) of each FAR in the chloroplast-deficient *Euglena* strain SM-ZK via electroporation of synthetic double-stranded RNA. Knockdown efficiency was confirmed by RT-PCR. Cells were cultured under aerobic conditions until the stationary phase, followed by a 6-hour hypoxic treatment, after which C28 levels were quantified. The results showed that the *far2_KD* strain exhibited a ~70% reduction in C28 synthesis compared to the control strain, indicating that FAR2 plays a major role in wax ester biosynthesis. Furthermore, fatty acid profiling of *far2_KD* cells revealed a marked accumulation of odd-chain fatty acids, with pentadecanoic acid (C15) and heptadecanoic acid (C17) levels increasing approximately 9-fold and 8-fold, respectively, relative to the control. These findings suggest that suppression of FAR2 not only impairs wax ester synthesis but also alters fatty acid metabolism, potentially promoting the synthesis of odd-chain fatty acids.

[1] Tomiyama, et al., Sci. Rep., 7: 13504, 2017 doi: 10.1038/s41598-017-14077-6.
[2] Yoshida, et al., BMC Genomics, 17:182, 2016 doi: 10.1186/s12864-016-2540-6.

Title: Bone Marrow derived Mesenchymal Stromal Cells Suppress Leukemia Cell Proliferation via Multimodal Paracrine Interactions

Rasel Md Rakibul Hasan[1], Yasuaki Oda[1], Miho Hattori[2], Jiahao Yang[1], Tsukimi Goto[3], Naoyo Kajitani[2], and Takeshi Taketani[1*]

1 Department of Pediatrics, Shimane University Faculty of Medicine, 89-1, Enya, Izumo, Shimane, 693-8501. m219431@med.shimae-u.ac.jp (RH), y-oda@med.shimae-u.ac.jp (YO), jiahao@med.shimane-u.ac.jp (YJ),

2 Regenerative Medicine Center, Shimane University Faculty of Medicine, 89-1, Enya, Izumo, Shimane, 693-8501. mhatt001@med.shimane-u.ac.jp (M.H), naokaji@med.shimane-u.ac.jp (NK)

3. Clinical Laboratory Division, Shimane University Hospital, 89-1, Enya, Izumo, Shimane, 693-8501. t.goto@med.shimane-u.ac.jp (TG)

* Correspondence : ttaketani@med.shimane-u.ac.jp; Tel.: +81-853-20-2216
E-mail of the presenting author: m219431@med.shimae-u.ac.jp

Background

The bone marrow niche, particularly mesenchymal stem/stromal cells (BM-MSCs), plays a pivotal role in leukemia pathophysiology, yet the mechanisms of healthy (non-leukemic) BM-MSC interactions with leukemia cells remain incompletely understood. We investigated paracrine and vesicle mediated mechanisms using healthy donor BM-MSCs against lineage - different leukemic cell lines.

Method

We evaluated the impact of human BM-MSCs on acute myeloid leukemia (HL-60), acute lymphoblastic leukemia (HAL-01), and chronic myeloid leukemia (KCL-22) cell lines on both direct system and indirect co-culture systems with 0.4 μm and 3 μm transwell inserts. Leukemic cell lines were cultured with isolated MSC-derived exosomes (MSC-Exos). Using both leukemic cell lines and BM-MSCs, we checked cellular proliferation/survival and comprehensive genetic expression.

Result

Healthy BM-MSCs consistently suppressed all three leukemia cell proliferation without cytotoxicity, but the effect was pore-size dependent: absent in HL-60 at 0.4 μm through soluble factors/small extracellular vesicles, yet present/amplified across all subtypes at 3 μm (allowing larger vesicles/protrusions) Isolated MSC-EXOs showed no significant impact, suggesting synergy with multimodal factors is required. RNA-seq revealed shared regulatory hubs (immune modulation, inflammatory cytokines [TNF, IFNG, IL6], AKT signaling) alongside lineage-specific programs: JAK/STAT-adhesion in ALL, cell cycle checkpoints in CML, granulocyte adhesion/trafficking in AML.

Conclusion

Healthy donor BM-MSCs exert multi-modal, short-term anti-proliferative effects on diverse leukemia lineages via complex paracrine-structural communication, converging on immune and AKT pathways despite subtype heterogeneity. These findings contrast with predominant pro-tumor reports and highlight the context-dependency of stromal-leukemia interactions, offering mechanistic insights into niche biology with implications for targeted therapies.

Genomic structure analysis of molecular marker genes involved in nervous system development and behavior in the freshwater snail *Biomphalaria glabrata*

Mahiro Itakura[1], Nicolas L. Anthoine[1] and Kouhei Oonuma[1]
[1]Faculty of Life and Environmental Sciences, Shimane University
a231006@matsu.shimane-u.ac.jp

Freshwater snails have a long history as model organisms in genetics, developmental biology, and behavioral neuroscience. However, molecular developmental genetics and molecular neurobiology in these organisms have been limited by technical difficulties in introducing exogenous genes, as well as by the disruption of embryonic development caused by egg capsule removal, which is required for genetic manipulation. Recently, we overcame these technical barriers in the freshwater snail *Biomphalaria glabrata* by establishing a microinjection-based gene delivery method and an embryo culture system that supports normal development even after egg capsule removal (Oonuma et al., *Science Advances*, 2025). Furthermore, we have established a highly efficient CRISPR-based genome editing system and successfully generated gene knockout snails for the first time in this species. These advances enable *B. glabrata* to be established as a novel model organism for developmental genetics and molecular neurobiology.

Like other mollusks, *B. glabrata* possesses a central nervous system with giant neurons that have large cell bodies, as well as camera-type eyes that are functionally analogous to those of vertebrates. Although *B. glabrata* is best known as the intermediate host of schistosomiasis and has been extensively studied in the context of infection and immunology, research on nervous system development and behavioral neurobiology has been largely unexplored due to the technical limitations described above. In addition, although the genome sequence of *B. glabrata* has been determined, gene annotation remains incomplete, and the genomic structures of genes essential for nervous system development and function are largely unknown.

In this study, we first determined the exon–intron structures of six genes critical for nervous system development, particularly eye development and neurotransmission (*Etr*, *Rx*, *Rhodopsin*, *vGlut*, *Th*, and *Tph*), using 5′ and 3′ rapid amplification of cDNA ends (RACE) and sequence analysis. Some of these genes have alternatively spliced isoforms. Notably, the number of *vGlut* isoforms differed remarkably between larval and adult stages. To further investigate the function of these genes, we performed CRISPR/Cas9-mediated gene disruption, and the world's first homozygous *Th* mutant snails were established. *Th* encodes tyrosine hydroxylase, an enzyme essential for dopamine biosynthesis. The *Th* mutant snails are expected to be dopamine-deficient and exhibited a marked reduction in egg-laying activity, suggesting a critical role of dopaminergic neurons in oviposition. These results open the door to future studies in developmental genetics and molecular behavioral neurobiology in *B. glabrata*. In future studies, we will elucidate the molecular basis of nervous system development and behavior through gene disruption and exogenous gene overexpression.

Element-Specific Atomic Structure Determination @ Shimane University

J. R. Stellhorn[1]
[1]Co-Creation Research Institute for Advanced Materials, Shimane University, Japan

jrstellhorn@mat.shimane-u.ac.jp

Element-specific determination of atomic structures is essential for elucidating the local environments that govern the functionality of advanced materials. Our lab employs a comprehensive suite of complementary, element-selective probes to achieve accurate and site-resolved structural analysis. Our approach integrates atomic-resolution X-ray holography, anomalous/resonant X-ray scattering, X-ray absorption spectroscopy and X-ray diffraction to resolve coordination geometry, bonding characteristics, electronic structure, and local disorder. By combining these techniques, we can map the atomic configurations around specific elements and detect subtle distortions. This presentation highlights recent developments and representative case studies for atomic-scale structure determination and their use in Materials Science: Bismuth silicate glasses with high dielectric permittivity[1], chalcogenide amorphous alloys exhibiting phase-change behavior[2,3], and an Fe_2VAl Heusler-type thermoelectric material[4]. These examples highlight how element-specific structural analysis reveals critical structure-property relationships, guiding the rational design of advanced functional materials.

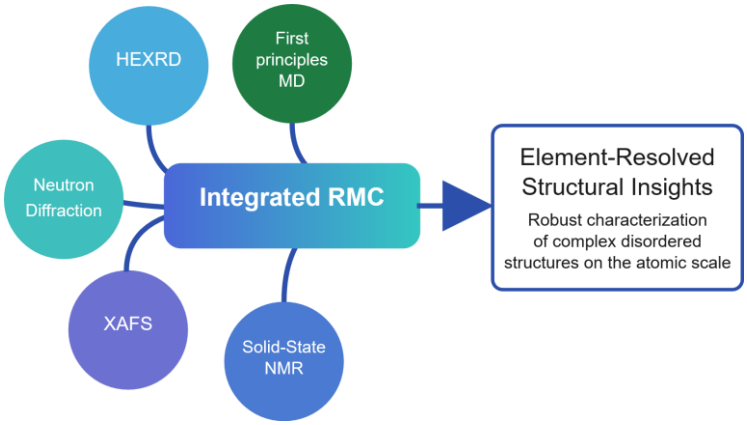

Fig. 1. Flowchart of the Reverse Monte Carlo (RMC) modelling approach with combined experimental and computational data for the characterzation of amorphous materials.

References

1) J.R. Stellhorn et al., *Phys. Rev. B* **113**, 014201 (2026)
2) J.R. Stellhorn et al., *J. Phys.: Condens. Matter* **35**, 304004 (2023)
3) J.R. Stellhorn et al., *Phys. Rev. B* **101**, 214110 (2020)
4) K. Kimura et al., Phys. Rev. B **101**, 024302 (2020).

Prediction of Electronic Conductivity in Perovskites Using Machine Learning

Yueyuan Gao[1], Takaya Fujisaki[1] and Kenji Yashiro[1, 2]
[1]Faculty of Materials for Energy, Shimane University
[2]Graduate School of Environmental Studies, Tohoku University
yueyuangao@mat.shimane-u.ac.jp

Electrochemical devices, such as all-solid-state batteries and solid oxide fuel cells, are anticipated as next-generation energy storage and conversion technologies. In these systems, coating layers play a critical role in maintaining interfacial stability, and their electronic conductivity strongly influences charge transport, performance, and long-term durability. This motivates the use of machine learning approaches to predict the electronic conductivity of perovskite materials across a wide compositional space. Inspired by the study of Schlenz *et al.* [1], we apply their k-nearest neighbors (kNN) framework to a dataset generated using Pecon.py and investigate its applicability to extended compositions.

Using $BaTiO_3$ as a benchmark, we demonstrate that strong correlations exist among structural features derived from lattice parameters. By performing feature selection guided by correlation analysis and validating the reduced feature space with principal component analysis, we obtain continuous and physically meaningful conductivity predictions (Fig. 1).

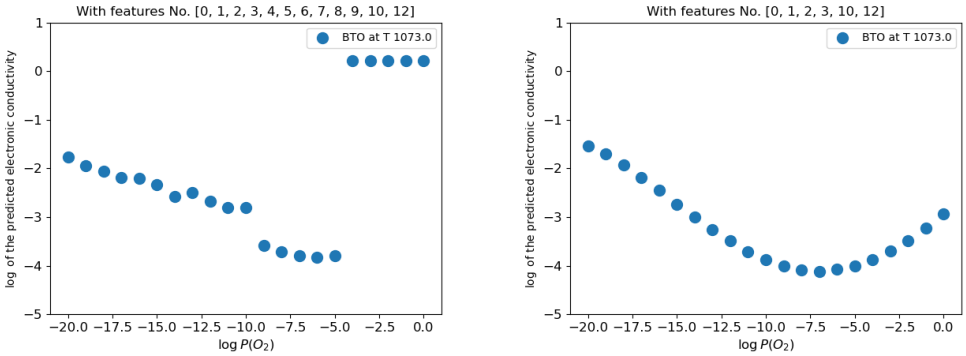

Figure 1: Comparison of kNN conductivity predictions before and after feature selection

We then apply the same framework to $BaCoO_3$, where the predicted conductivity becomes discontinuous. This behavior is attributed to extrapolation beyond the dataset's coverage, particularly because the B-site Co ionic radius lies outside the effective range of the dataset.

Based on these observations, we define an effective region in feature space within which kNN-based predictions can be considered physically reliable. Our results highlight both the usefulness and the limitations of local machine learning models for materials property prediction and provide guidance for assessing prediction reliability in perovskite conductivity studies.

Reference

[1] Schlenz, H.; Baumann, S.; Meulenberg,W.A.; Guillon, O., The Development of New Perovskite-Type Oxygen Transport Membranes Using Machine Learning. *Crystals* 2022, 12, 947. https://doi.org/10.3390/cryst12070947

Photoluminescence behaviour of Eu3+-doped Layered double hydroxide for nitrate detection ability.

Fatima Zoha, Takuya Fujimura and Ryo Sasai
Faculty of Materials for Energy, Shimane University
n24m644@matsu.shimane-u.ac.jp

【Introduction】Nitrate anions in water are known as a kind of toxic anion species because of their adverse effects on the aquatic environment and living organisms. Selective detection and efficient removal of nitrate anions from water is a critical issue for compliance with the international water standard. In this study, I synthesized chloride type LDH consisting of Mg and Al with 3% Eu^{3+} doping at the Al site as a luminescence rare-earth cation (Eu-LDH(Cl)) and investigated its nitrate selectivity in pure and sea water and detection performance by photoluminescence changes.

[Experiment] Eu-LDH(CO_3) was synthesized by hydrothermally treating reaction solution ([Mg^{2+}] = 100, [Al^{3+}] = 48.5, [Eu^{3+}] = 1.5, and [hexamethylenetetramine] = 175 mmol/L) at 140℃ for 24 h[7]. Eu-LDH(Cl) as starting materials for anion-exchange experiment from chloride to nitrate was prepared by HCl-EtOH decarbonate method[2]. Anion exchange experiments from chloride to nitrate anions in pure and sea water were carried out by dispersing Eu-LDH(Cl) in solution of $NaNO_3$ and NaCl with various mixed ratios. Characterization of all samples was conducted by XRD, FT-IR, ICP-AES, IC, diffuse reflectance spectroscopy, and photoluminescence spectroscopy.

[Result & Discussion] In Fig. 1, Photoluminescence (PL) spectra of Eu-LDHs with carbonate and chloride anions are shown. From PL spectra, both Eu-LDH with carbonate and chloride anions showed Eu^{3+} derived luminescence. A decrease in PL intensity was observed when anion species in the interlayer of Eu-LDH was changed from carbonate to chloride anions. The reason for this decrease in PL intensity is still unclear.PL spectra measurements of Eu-LDH obtained after anion-exchange experiments from chloride to nitrate anions showed PL quenching depending on the initial nitrate concentration. These results suggest that the Eu-LDH is a promising material that can detect nitrate ions by changes in PL intensity. The PL intensity ratio of $^5D_0 \rightarrow {}^7F_2$ and $^5D_0 \rightarrow {}^7F_1$ transitions ($I(^5D_0 \rightarrow {}^7F_2)/I(^5D_0 \rightarrow {}^7F_1)$) was plotted against the initial nitrate concentration in Fig. 2 [7]. This result indicates that Eu-LDH(Cl) can be used to quantitatively detect the concentration of nitrate anion in water using the $I(^5D_0 \rightarrow {}^7F_2)/I(^5D_0 \rightarrow {}^7F_1)$ values.

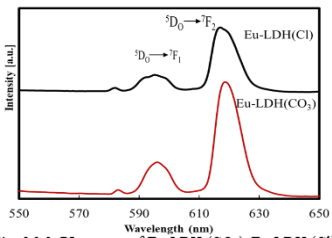

Fig. 3.2.2. PL spectra of Eu-LDH (CO_3), Eu-LDH (Cl) (1/3).

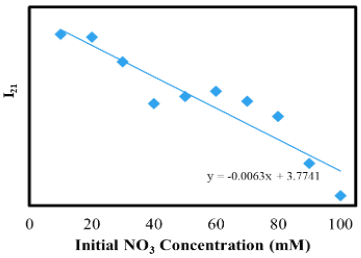

Fig. 3.3.2.2. I_{21} Spectra of Eu-LDH (1/3)

References: 1) Sasai, R. et al., Luminescence 2025, 40: e70174.
2) Chen, Y.; et al., *J. Solid State Chem.* **2010**, *183*, 2222.
3) Iyi, N.; et al., *Appl. Clay Sci.* **2011**, *54*, 132.

Clinical evaluation of a novel cotton-like β-TCP/PLLA/PGA bone graft material for jaw bone defects following cystectomy

Tomohiko Doigami[1], Yuhei Matsuda[1], Michitaka Somoto[1], Reon Morioka[1,2], Rie Osako-Sonoyama[1], Hiroto Tatsumi[1,3], Masako Fujioka-Kobayashi[1], Takahiro Kanno[1]
[1]Department of Oral and Maxillofacial Surgery, Shimane University Faculty of Medicine, Izumo, Shimane, Japan
[2]Department of Pharmacology, Shimane University Faculty of Medicine, Izumo, Shimane, Japan
[3]Innovative Cancer Center, Shimane University Hospital, Izumo, Shimane, Japan
E-mail of the presenting author: den.d.tomohiko@med.shimane-u.ac.jp

Abstract

Objectives: Jaw bone defect following jaw bone cystectomy may cause some postoperative complications such as pathological fracture and secondary infection. Therefore, various bone grafting has been conducted. Novel cotton-like bone graft material composed of β-TCP/PLLA/PGA has handling properties, three dimensional shapeability and bone formation and is considered to have potential clinical utility for bone formation. However, no studies have evaluated the clinical outcomes of this novel β-TCP/PLLA/PGA in patients of oral and maxillofacial surgery. Thus, this study aimed to evaluate the usefulness of β-TCP/PLLA/PGA in bone regeneration within jaw bone defects following cystectomy.

Patients and Methods: 28 Patients (19 males and 9 females; mean age: 47.5 years) who visited the Department of Oral and Maxillofacial Surgery, Shimane University Hospital, between November 2022 and April 2024, underwent cystectomy for bimaxillary jaw bone dentigerous cysts, and were grafted with β-TCP/PLLA/PGA were included. Patient demographics, clinical data, and CT images were retrospectively evaluated to assess jaw bone defects (defect dimensions, CT values, and bone continuity). Postoperative complications were obtained from medical records.

Results: Both the long and short axis lengths of the jaw bone defect showed a significant decrease at 6-months postoperatively compared with the preoperative values and those at 1 month postoperatively. CT values showed a significant increase from 1-month to 6-months postoperatively ($P<0.05$). At the 6-months postoperatively, 39.3% of cases obtained full bone continuity. No serious adverse events were observed.

Conclusions: β-TCP/PLLA/PGA demonstrated excellent handling characteristics and clinical safety as a novel cotton-like bone graft material for jaw bone defects following cystectomy.

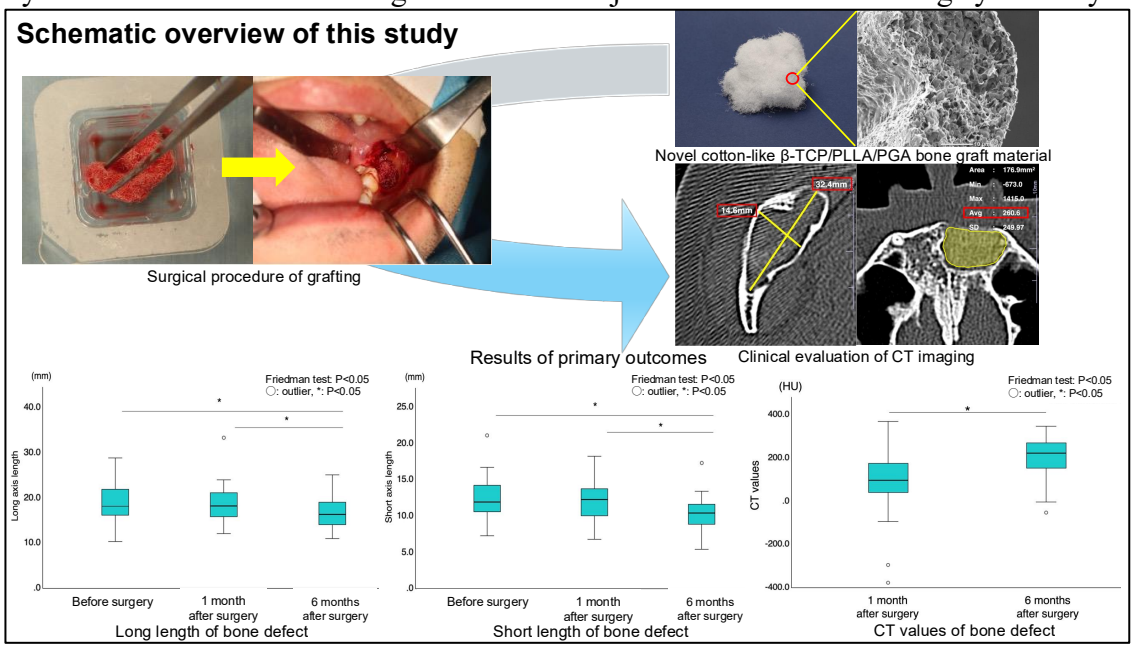

Medical Application of Electrical Impedance Tomography (EIT) and Current Induced Magnetic Tomography (CIMT)

Yoshiaki Iwashita[1,2], Satoru Nebuya[3,4]
[1]Head Office for Regional Collaboration and Innovation, Shimane University
[2]Emergency and Critical Care Medicine, School of Medicine, Shimane University
[3]Joint Research Chair for Advanced Medical Electromagnetic Engineering, Shimane University
[4]POSH WELLNESS LABORATORY Inc.
iwaci1ta@med.shimane-u.ac.jp

Electrical impedance tomography (EIT) is a noninvasive imaging technique that reconstructs cross-sectional images by injecting weak electrical currents and measuring resulting impedance changes. A major advantage of EIT is that it enables radiation-free and continuous imaging at the bedside. In recent years, EIT has become commercially available in critical care settings, particularly for evaluating and optimizing mechanical ventilator settings. However, currently available EIT systems have several limitations, including acquisition of only a single cross-sectional plane and the need for direct attachment of multiple electrodes to the patient.

To overcome these limitations, we have developed a novel EIT system capable of simultaneously acquiring four cross-sectional planes, using eight electrodes per section. The reconstructed images are further integrated to generate three-dimensional (3D) images. Using this system, we successfully obtained 3D images from patients with pneumonia and lung cancer in the emergency department of Shimane University Hospital (Fig).

In addition, we have developed a new imaging technique that detects changes in magnetic fields induced by applied electrical currents, enabling non-contact tomographic imaging of internal structures within electrically insulating objects. We refer to this technique as current-induced magnetic tomography (CIMT). As an initial application, we developed a CIMT system to detect blood clot formation in artificial lungs used in extracorporeal membrane oxygenation (ECMO) circuits.

Future applications of CIMT include cerebral imaging in ambulances for early stroke detection and whole-body scanning for the early detection of malignancies. In this presentation, we introduce these novel imaging technologies and discuss their potential applications in various medical fields.

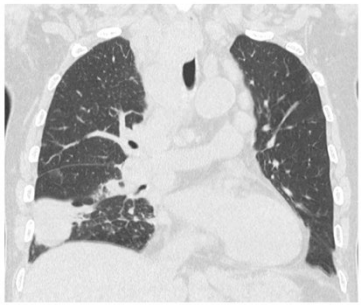

CT image

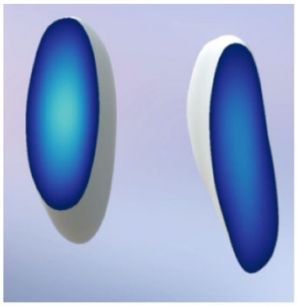

EIT image

Biochemical analysis of the interaction site between SARS-CoV-2 RNA helicase nsp13 and RNA-dependent RNA polymerase nsp12

Moushumi Akter, Shunpei Okada, Masami Wada, Hisashi Iizasa
Department of Microbiology, Faculty of Medicine, Shimane University
m249611@med.shimane-u.ac.jp

[**Background**] Severe acute respiratory syndrome coronavirus 2 (SARS-CoV-2) is an enveloped, positive-sense, single-stranded RNA virus and the causative agent of coronavirus disease 2019 (COVID-19) and Long COVID. While several antiviral drugs for COVID-19 have been approved, the emergence of resistant strains necessitates the identification of novel therapeutic strategies. The SARS-CoV-2 RNA-dependent RNA polymerase (RdRp), nsp12, forms a complex with cofactors nsp7 and nsp8 to facilitate viral RNA replication and transcription. Recent cryo-electron microscopy (cryo-EM) analyses suggest that this RdRp complex interacts with the viral RNA helicase, nsp13, in an RNA-dependent manner. This study focuses on the specific interaction interface between the RdRp subunit nsp12 and nsp13, involving four conserved residues on nsp13 (L92, Y93, K94, and N95). Our previous data indicated that an alanine substitution of four amino acids (4A) at this nsp12–nsp13 interaction interface abolishes viral replication and subgenomic RNA synthesis. However, it remained unclear whether this inhibition resulted from a defect in the enzymatic activity of nsp13 or the loss of the interaction itself.

[**Method**]Using an *E. coli* expression system, we purified wild-type nsp13 and the nsp13 4A mutant. The nsp12–nsp7–nsp8 complex was prepared similarly. Helicase activity was measured using nsp13 ATPase assay and double-stranded RNA (dsRNA) unwinding assay, while the binding affinity to the RdRp complex was evaluated via electrophoretic mobility shift assay (EMSA).

[**Result**]ATPase assay demonstrated that the nsp13-4A mutant maintains RNA-dependent ATPase activity comparable to WT, despite a slight reduction. Similarly, the dsRNA unwinding assay confirmed that the mutant preserves its intrinsic helicase activity, with unwinding levels comparable to WT. However, electrophoretic mobility shift assays (EMSA) revealed that while WT nsp13 forms a complex with RdRp and dsRNA, the nsp13-4A mutant fails to bind the RdRp complex.

[**Discussion**]These findings conclude that the nsp12-nsp13 interface is not essential for enzymatic activity but is critical for the physical assembly of the RTC. Therefore, targeting this virus-specific interface offers a promising strategy for developing highly selective, broad-spectrum antiviral drugs that minimize off-target effects on host helicases and remain effective against future coronavirus variants. Moreover, this strategy, by potently suppressing subgenomic RNA synthesis, offers potential therapeutics for persistent infections such as Long COVID.

Parental socioeconomic status and medical specialty choice: a nationwide analysis of Japanese physicians

Kota Sakaguchi[1]
[1]General Medicine Center, Shimane University Hospital, 89-1 Enya-cho, Izumo, Shimane 693-8501, Japan
sakaguchi@med.shimane-u.ac.jp

Purpose of the study: Previous studies have suggested a potential link between parental socioeconomic status and medical specialty choice; however, empirical evidence from Japan remains scarce. Therefore, we aimed to investigate the association between parental socioeconomic status and medical specialty choice in Japan.

Study design: This nationwide cross-sectional online survey was conducted in June 2022 using "Nikkei Medical Online", a professional platform for physicians. Data on medical specialty choice and parental socioeconomic status indicators (household income, occupation, and birthplace) were collected. Parental socioeconomic status was dichotomized based on an annual household income threshold of US$60,000 (approximately 10 million JPY). Association was evaluated by multivariable logistic regression analysis.

Results: Of 3,580 physicians included, 48.6% were from families with a parental household income of US$60,000 or more. The proportion of physicians from high-income families was the highest in neurosurgery (65.8%) and dermatology (57.0%) and the lowest in radiology (30.8%), pathology (36.2%), and psychiatry (35.7%). Using multivariable analysis, choosing certain specialties was significantly associated with having a physician father (adjusted odds ratio, 14.46; 95% confidence interval, 12.10–17.29) and being born in an urban area (adjusted odds ratio, 1.65; 95% confidence interval, 1.41–1.92).

Conclusions: This is the first study to quantitatively assess the significant association between parental socioeconomic status and medical specialty choice among physicians in Japan. Parental socioeconomic status appears to be a key factor in physicians' career choices. Future research should be more comprehensive and include multifaceted components of socioeconomic status and psychosocial factors.

Title: Roles of Ripasudil on Schlemm's Canal Morphology in The Tissues Obtained During Trabeculectomy

Aysha Siddika Mukta[1], Aika Tsutsui[1], Teruhiko Hamanaka[2], Sachiko Kaidzu[1], Kanae Kobayashi[2], Nobuo Ishida[3], Masaki Tanito[1 *]
[1] Department of Ophthalmology, Faculty of Medicine, Shimane University, Izumo, Japan
[2] Department of Ophthalmology, Japanese Red Cross Hospital Medical Center, Tokyo, Japan
[3] Department of Ophthalmology, Ishida Eye Clinic, Joetsu, Japan
E-mail: m259401@med.shimane-u.ac.jp

Purpose: To evaluate the effects of preoperative topical ripasudil, a Rho-associated protein kinase (ROCK) inhibitor, on Schlemm's canal (SC) morphology in patients with primary open-angle glaucoma (POAG).

Methods: This retrospective study included 95 SC specimens obtained during trabeculectomy from 95 patients with POAG. Based on preoperative treatment, patients were divided into two groups: ripasudil (-) group (n = 68) receiving four topical medications [FP receptor agonist, β-blocker, carbonic anhydrase inhibitor (CAI), and α_2 agonist], and ripasudil (+) group (n = 27) receiving the same four medications plus ripasudil. SC morphology parameters were assessed in thrombomodulin (TBM)-stained sections, including length parameters [TBM-positive/negative and opened/closed SC lengths] and area parameters [TBM-positive/negative and opened SC areas]. Between-group comparisons were performed using unpaired t-tests, and multiple regression analysis was conducted to adjust for age, gender, preoperative intraocular pressure (IOP), and oral CAI use.

Results: The ripasudil (+) group had significantly longer total SC length (TSC: 302.5 μm) than the ripasudil (-) group (273.0 μm, p = 0.023). Among area parameters, the ripasudil (+) group showed significantly larger opened SC area (OSC-A: 2689 μm² vs. 1881 μm², p = 0.008) and TBM-negative opened SC area (NOSC-A: 554 μm² vs. 299 μm², p = 0.001), whereas TBM-positive opened SC area (POSC-A) was not significantly different between groups (2001 μm² vs. 1575 μm², p = 0.096). After multivariate adjustment, ripasudil use remained significantly associated with longer TSC (p = 0.011) and larger OSC-A (p = 0.014) and NOSC-A (p = 0.001).

Conclusions: Preoperative topical ripasudil use was associated with preservation of SC lumen morphology, particularly in regions lacking SC endothelium. These findings suggest a potential role of ROCK inhibitors in maintaining SC structure and function in glaucoma.

Keywords: Primary open-angle glaucoma; Rho-associated protein kinase inhibitor; Ripasudil; Schlemm's canal morphology; Trabecular meshwork; Aqueous humor outflow

Effects of *Desulfovibrio piger* on Caco-2 cell viability as an *in vitro* model of inflammatory bowel disease

Nitchatorn Sungsirin[1], Masami Wada[1], Shunpei Okada[1], and Hisashi Iizasa[1]
[1] Department of Microbiology, Faculty of Medicine, Shimane University
m239424@med.shimane-u.ac.jp

Abstract

Desulfovibrio piger has been increasingly implicated in the pathogenesis of inflammatory bowel disease (IBD). However, its direct effects on intestinal epithelial cells remain incompletely understood. This study investigated the impact of *D. piger* on Caco-2 cell viability using an anaerobic *in vitro* coculture model. Growth kinetics of *D. piger* in Modified Barr's medium identified a clear logarithmic phase between 12 and 60 h, during which optical density (OD_{600}) showed a strong linear correlation with viable cell counts (CFU/mL), enabling accurate preparation of defined multiplicities of infection (MOIs). Caco-2 cells maintained high viability under anaerobic conditions for up to 48 h, validating the experimental setup. Anaerobic coculture with *D. piger* resulted in a significant, MOI- and time-dependent reduction in Caco-2 cell viability, with markedly greater cytotoxicity observed at 24 h compared with 12 h. Integrated dose–response analysis demonstrated a strong inverse linear relationship between bacterial load and epithelial cell survival. Compared with *Escherichia coli*, *D. piger* induced significantly greater epithelial damage at equivalent MOIs. Notably, exposure to dead *D. piger* did not reduce Caco-2 cell viability, whereas living bacteria caused substantial cytotoxicity, indicating that epithelial injury is mediated by metabolically active bacterial processes rather than structural components alone. These findings suggest that secreted factors or metabolites derived from *D. piger* play a critical role in epithelial damage and warrant further investigation. Overall, this study establishes a reproducible *in vitro* model to elucidate *D. piger* - host interactions relevant to IBD pathogenesis.

Keywords: *Desulfovibrio piger,* Inflammatory bowel disease, Caco-2 cell, Coculture, Cytotoxicity, Cell viability

MCR-LIME: Component-Level Interpretability of Machine Learning Models for Raman Spectroscopy-Based Breast Cancer Cell Classification

Mengxin Yang[1], Tatsuyuki Yamamoto[2] and Hemanth Noothalapati[2]
[1]Graduate School of Natural Science and Technology, Shimane University
[2]Faculty of Life and Environmental Sciences, Shimane University
n24m827@matsu.shimane-u.ac.jp

Raman spectroscopy is a label-free and noninvasive technique that provides rich molecular fingerprint information at the single-cell level, making it a promising tool for cancer cell classification. However, the high dimensionality and severe spectral overlap of biological Raman data limit not only classification reliability but also the interpretability of machine learning models. In this study, we developed a component-level explainable framework, termed MCR-LIME, which integrates multivariate curve resolution–alternating least squares (MCR-ALS) with local interpretable model-agnostic explanations (LIME) to interpret machine learning–based classification models for single-cell Raman spectroscopy of breast cancer cells.

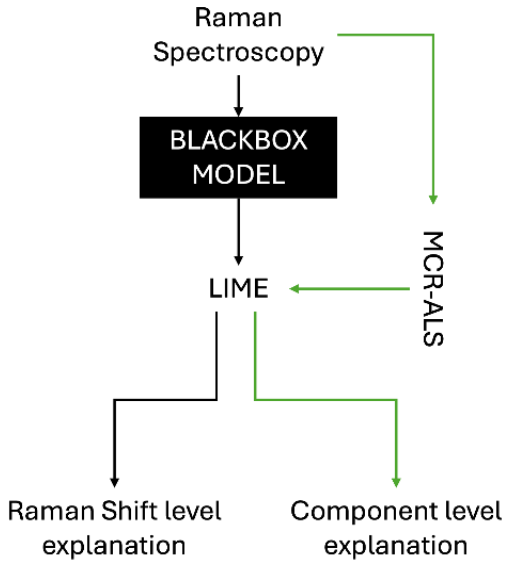

Figure 1. Conceptual comparison of interpretation pathways

As illustrated in Figure 1, conventional interpretation pipelines (black arrows) are limited to wavenumber-level explanations, whereas the incorporation of the developed framework (green arrows) enables chemically meaningful, component-level interpretation.

To validate the applicability of MCR-LIME, multiple classifiers, including rbf-SVM, linear SVM, random forest, XGBoost, and LightGBM, were first constructed using single-cell Raman spectra of normal human mammary epithelial cells (HMEpC) and breast cancer cells (MCF-7) and evaluated by group-wise cross-validation. All models achieved classification accuracies around 90%, indicating that the trained classifiers provide a reliable basis for interpretability analysis. Subsequently, MCR-ALS was applied to decompose the Raman spectra into eight chemically interpretable components, including proteins, glycoproteins, linoleate-rich triglycerides, and background water signals, serving as a biochemical foundation for component-level interpretation. Compared with conventional SHAP and LIME methods that focus on individual wavenumbers, MCR-LIME enables both local and global interpretation at the molecular component level, revealing that cancer cell predictions are mainly associated with decreased glycoproteins and linoleate-rich triglycerides and increased protein-related components, consistent with known metabolic reprogramming in breast cancer cells. Furthermore, MCR-LIME reveals that certain models rely partially on background water signals, an effect that is difficult to detect using conventional wavenumber-level explanation methods.

Rapid Label-Free Detection of UTI Pathogens Using Raman Spectroscopy

Sri Surya Charan Kondeti[1], Richik Roy Choudhury[2], Suhanya Duraiswamy[2], Tatsuyuki Yamamoto[3] and Hemanth Noothalapati[3,*]

[1]The United Graduate School of Agricultural Sciences, Tottori University, Japan
[2]Department of Chemical Engineering, Indian Institute of Technology Hyderabad, India
[3]Faculty of Life and Environmental sciences, Shimane University, Japan

E-mail: [d25a2005@matsu.shimane-u.ac.jp]

Introduction: Urinary tract infections (UTIs) are among the most common bacterial infections globally. Conventional culture-based diagnosis requires 24-72 hours, often leading to empirical antibiotic administration that contributes to antimicrobial resistance. There is a critical need for rapid, label-free diagnostic alternatives to enable timely targeted therapy. This study evaluates Raman spectroscopy combined with machine learning as a non-destructive method to capture molecular fingerprints of uropathogens for automated discrimination.

Experimental Conditions: Raman spectra were acquired from representative Gram-positive (*Bacillus subtilis*, *Staphylococcus aureus*) and Gram-negative (*Escherichia coli* UTI89, *E. coli* DH5α, *Proteus mirabilis*) bacterial species. Raman spectra were recorded using a LabRAM HR Evol system with 532 nm excitation, a 100× objective, and a 600 grooves mm^{-1} grating. Spectra were acquired with 15 s integration time and four accumulations under identical measurement conditions for all bacterial species.

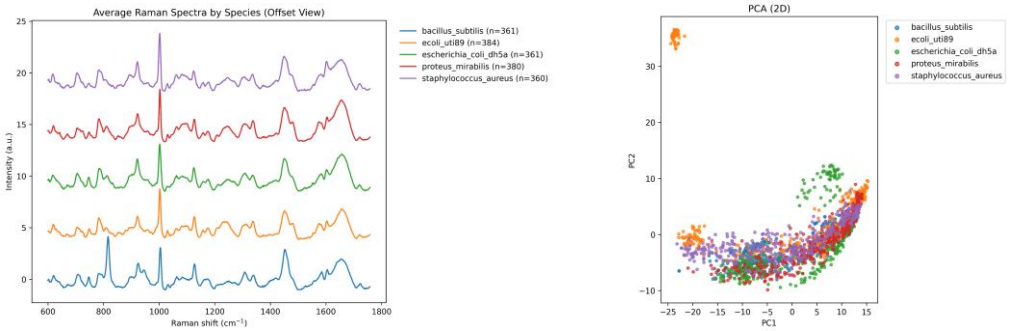

Figure 1A. Average Raman spectra by species. 1.B Two-dimensional PCA projection of Raman spectra.

Results and Discussion: Average spectra show species-wise Raman features (Fig. 1A). PCA reveals clear species-level clustering (Fig. 1B), showing distinct spectral fingerprints despite partial biochemical overlap. Machine learning effectively captured multivariate spectral relationships, demonstrating the feasibility of rapid, label-free UTI pathogen detection and its potential for portable point-of-care diagnostics.

Evaluation of bone regenerative and bioactive potential of β-TCP/PLLA/PGA nanobiomaterial in conjunction with concentrated conditioned media from rapidly expanding clone (REC) of mesenchymal stem cells: A pilot animal study

Ankhtsetseg Shijirbold[1], Mrunalini Ramanathan[1], Masako Fujioka-Kobayashi[1], Nithish Sankepally[1], Yuhei Matsuda[1], Yumi Matsuzaki[2], Yuki Fujita[3], Takahiro Kanno[1*]

[1] Department of Oral and Maxillofacial Surgery, Shimane University Faculty of Medicine, Izumo, Shimane, Japan

[2] Department of Life Science, Shimane University Faculty of Medicine, Izumo, Shimane, Japan

[3] Department of Developmental Biology, Shimane University Faculty of Medicine, Izumo, Shimane, Japan

E-mail: m239403@med.shimane-u.ac.jp

Abstarct

Maxillofacial bone defects pose significant reconstructive challenges due to their functional and esthetic consequences. Although mesenchymal stem cells (MSCs) have been explored for bone regeneration, their clinical application is limited by technical and immunogenic concerns. Rapidly expanding clones (RECs), a superselected MSC variant, and their conditioned media (REC-CM) offer a promising cell-free regenerative strategy.

This study evaluated the bone regenerative potential of a β-tricalcium phosphate/poly-L-lactic acid/polyglycolic acid (β-TCP/PLLA/PGA) nanobiomaterial scaffold combined with REC-derived conditioned media. Plain CM, 1× concentrated REC-CM, and 10× concentrated REC-CM were prepared, and growth factor levels were quantified using ELISA. Critical-sized mandibular defects were created in rats and treated with scaffold implantation combined with each CM formulation. Bone regeneration was assessed at weeks 1 and 4 using bone volume-to-total volume (BV/TV), bone mineral density (BMD), defect margin regrowth, and immunohistochemical analysis of osteogenic and bioactive markers.

The 10× REC-CM group demonstrated significantly elevated levels of angiogenic factors, including TGF-β1 and VEGF, indicating enhanced vascularization. This group showed markedly higher BV/TV at week 4 and increased new bone formation within the defect region at both time points compared with the other groups. Furthermore, osteogenic markers such as Runx2, LepR, osteocalcin, and periostin were significantly upregulated in the 10× REC-CM group, confirming strong osteoinductive activity.

These findings demonstrate that concentrated REC-derived conditioned media synergistically enhance the osteogenic performance of β-TCP/PLLA/PGA scaffolds. The application of 10× REC-CM promotes early-phase bone regeneration and represents a promising strategy for maxillofacial and bone tissue reconstruction.

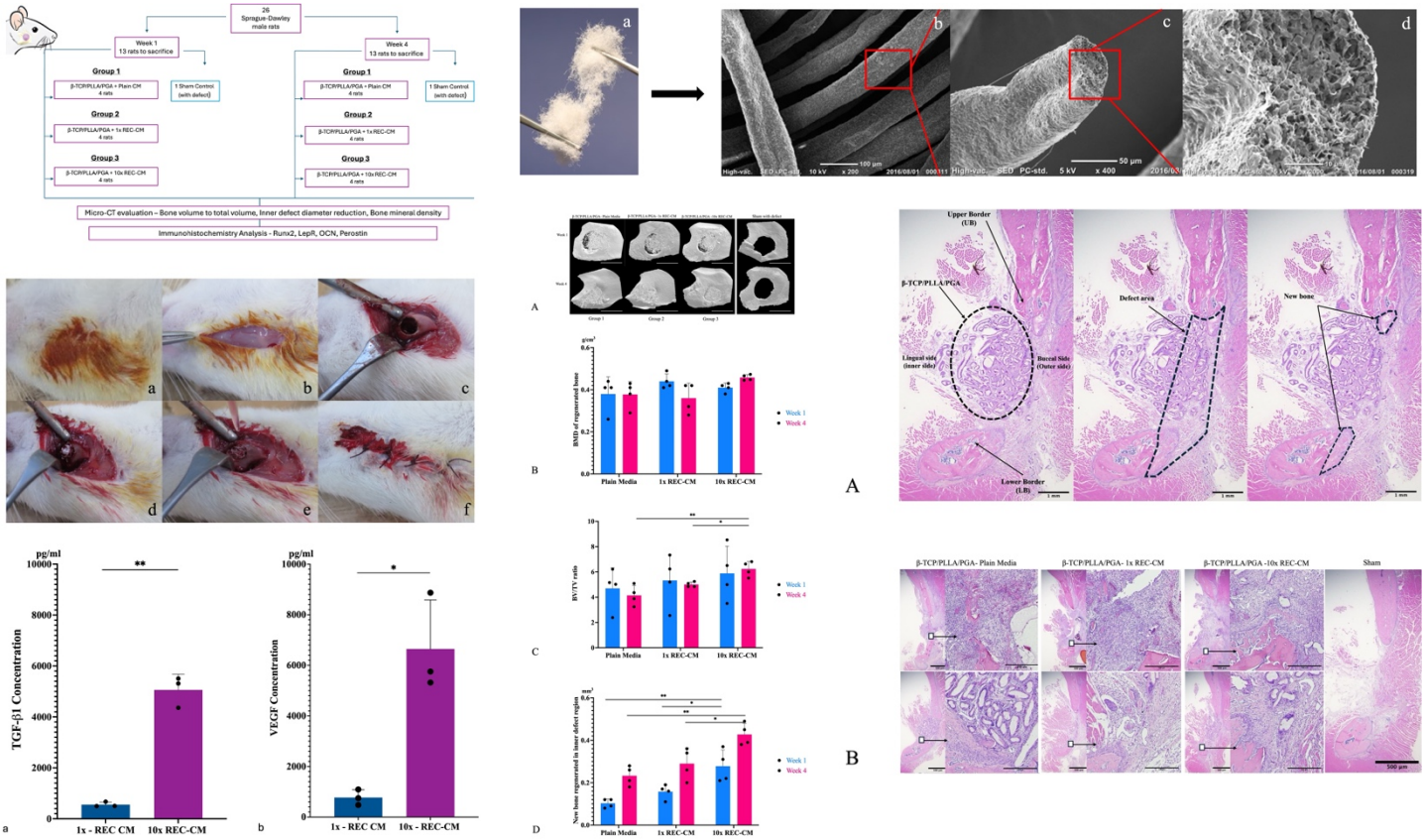
26 Sprague-Dawley male rats
Week 1 13 rats to sacrifice
Week 4 13 rats to sacrifice
Group 1
β-TCP/PLLA/PGA + Plain CM 4 rats
1 Sham Control (with defect)
Group 2
β-TCP/PLLA/PGA + 1x REC-CM 4 rats
Group 3
β-TCP/PLLA/PGA + 10x REC-CM 4 rats
Micro-CT evaluation – Bone volume to total volume, Inner defect diameter reduction, Bone mineral density
Immunohistochemistry Analysis - Runx2, LepR, OCN, Perostin
A
a
b
c
d
B
e
f
A
B
C
D
BMD of regenerated bone
RV/TV ratio
New bone regenerated in inner defect region
Week 1
Week 4
Plain Media
1x REC-CM
10x REC-CM
TGF-β1 Concentration
VEGF Concentration
pg/ml
1x - REC CM
10x REC-CM
10x - REC-CM
Upper Border (UB)
β-TCP/PLLA/PGA
Defect area
New bone
Lingual side (inner side)
Buccal Side (Outer side)
Lower Border (LB)
β-TCP/PLLA/PGA- Plain Media
β-TCP/PLLA/PGA- 1x REC-CM
β-TCP/PLLA/PGA -10x REC-CM
Sham
4x
20x
40x
RUNX2 expression IHC Score
LepR expression IHC Score
OCN expression IHC Score
Periostin expression IHC Score

A scheme of harmonics mitigating in windfarm using doubly fed induction generator turbine used with Shunt active power filter equip automatic fuzzy gain controller.

Izumi Kadowaki[1], Izumi Kadowaki[1]
[1]Shimane university
n25m308@matsu.shimane-u.ac.jp

Recent years, power electronic devices are used in various situation and location. Especially, in grid connected place, since converter devise's switch and resonance phenomena caused by inductive component and capacitive component in entire circuit, Harmonics; High order frequent noises are generated. It can distort voltage and current, and if THD; Total Harmonic Distortion over specified value, electric device may be damaged significantly. Therefore here, for stable power generate and keep safety grid connection, a scheme of harmonic mitigating will propose in model composed on Simulink/MATLAB. Here, taking wind farms using doubly fed induction generator turbine as an example.

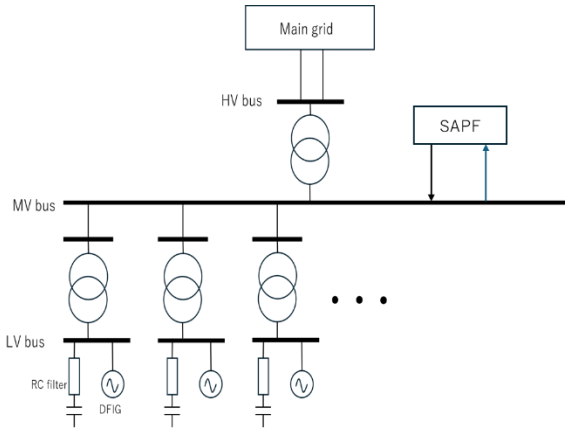

Figure 1 Model of wind farm with SAPF

As shown in Figure 1, the connection between the entire wind farm and the grid is depicted. Here, a Shunt Active Power Filter (SAPF) is introduced at the medium-voltage bus—the point where noise generated by each wind turbine is consolidated—to autonomously reduce harmonics. The results are shown in Figure 2.

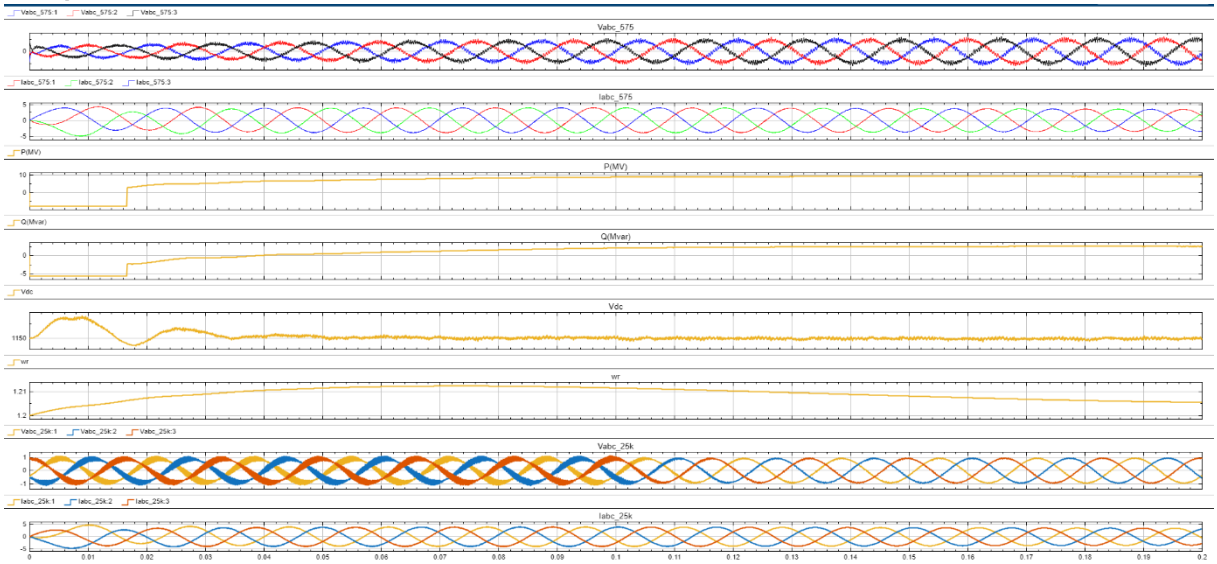

Figure 2 Result of harmonic mitigating control

Reference: A Comprehensive Analysis Study about Harmonic Resonances in Megawatt Grid-Connected Wind Farms, 19-22 Oct 2014 [1]

Experimental Analysis of High-Frequency Switching Waveforms in GaN-FET based Inverter

Md Naeem Hussain[1], Xupeng Dong[2], Associate Prof. NGUYEN Gia Minh Thao[3]
[1]Department of Mechanical, Electrical and Electronic Engineering, Shimane University,
[2]Department of Mechanical, Electrical and Electronic Engineering, Shimane University,
[3]Department of Mechanical, Electrical and Electronic Engineering, Shimane University,
Japan.
n24m329@matsu.shimane-u.ac.jp

Abstract

This study aims to assess a GaN-FET-based inverter's high-frequency switching performance experimentally. Conventional silicon devices face significant switching losses and waveform degradation at high frequencies, which limits inverter operation in the MHz range. To address this problem, a GaN half-bridge inverter driven by a high-speed gate driver and controlled using a dsPIC-based PWM controller was implemented. To examine voltage stability, waveform quality, and switching behavior, experimental switching waveforms were measured at 500 kHz and 1 MHz with only a minor increase in ripple and noise at 1 MHz, the results display stable rectangular output waveforms at both frequencies. These findings confirm that GaN-FET inverters are well suited for high-frequency power conversion and demonstrate reliable operation up to 1 MHz.

Figure 1 illustrates the overall configuration of the GaN-based inverter system used for high-frequency switching experiments, including the control unit, gate driver, power stage, and feedback circuits.

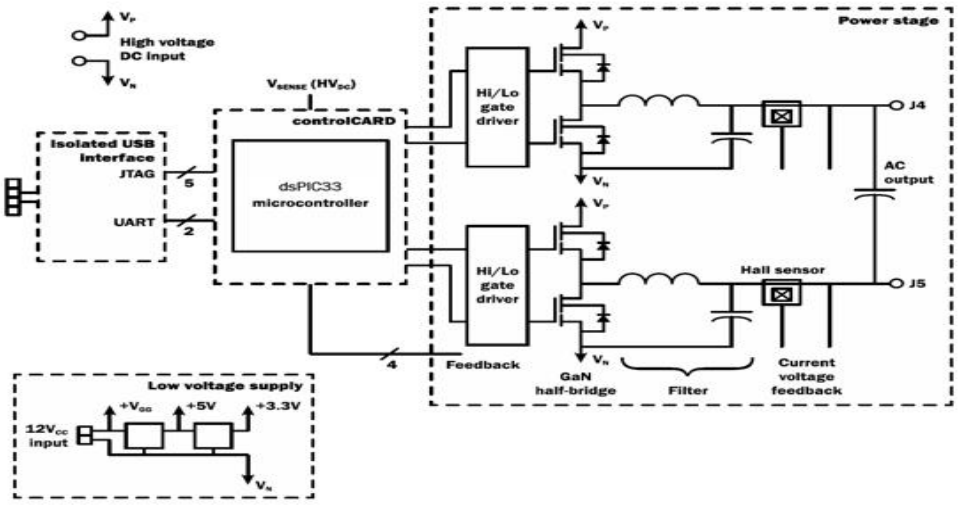

Figure 1: GaN-based inverter system for high-frequency switching evaluation [1]

Table 1: Comparison of Experimental Switching Performance

Parameter	500 kHz Operation	1 MHz Operation
Switching frequency	500 kHz	1 MHz
Switching period	2.0 µs	1.0 µs
Output voltage level	Stable (~3.3–3.5 V)	Stable (~3.3–3.5 V)

Reference

[1] Microchip Technology Inc., "TIDM3000-W050B GaN-Based Inverter Evaluation Kit," Available: https://www.microchip.com/tdinv3000w050b-kit.

Machine Learning Models for Battery State-of-Charge Estimation in Dynamic Load and Temperature Change

Huynh Tran Minh Tri[1], La Phuong Ha[2], Ton That Long[3] and Nguyen Gia Minh Thao[1]

[1] Division of Mechanical, Electrical and Electronic Engineering, Graduate School of Natural Science and Technology, Shimane University, Matsue City, Japan
[2] Process Automation C&T Division, Pepperl+Fuchs Group, Ho Chi Minh City, Vietnam
[3] School of Electrical Engineering, International University, Vietnam National University – Ho Chi Minh City, Vietnam
n25d102@matsu.shimane-u.ac.jp

In today's modern world, under exponential development, energy consumption is also increasing. This leads to many environmental consequences due to the ever-increasing amount of emissions. Simultaneously, people have been researching to find cleaner energy sources and energy storage technologies. Currently, lithium-ion batteries (LIBs) are one of the most optimal components in energy conversion of energy storage systems (EMS) [1]. However, LIBs also pose a huge danger if the state is misdiagnosed. Accurate State-of-Charge (SoC) diagnosis can optimize the full potential of LIBs and protect the environment. In this study, we have been developing a method to estimate the SoC of LIBs using Artificial Intelligence (AI) as depicted in Figure 1. With only Voltage, Current, and Temperature as inputs, the Transformer model delivered impressive results with an RMSE below 1.63% over a wide temperature range from -10°C to 40°C. Furthermore, our comparison with current model-based research using the same inputs showed superior performance across the board. This demonstrates the Transformer model's reliability and makes it a strong contender for future BMS systems.

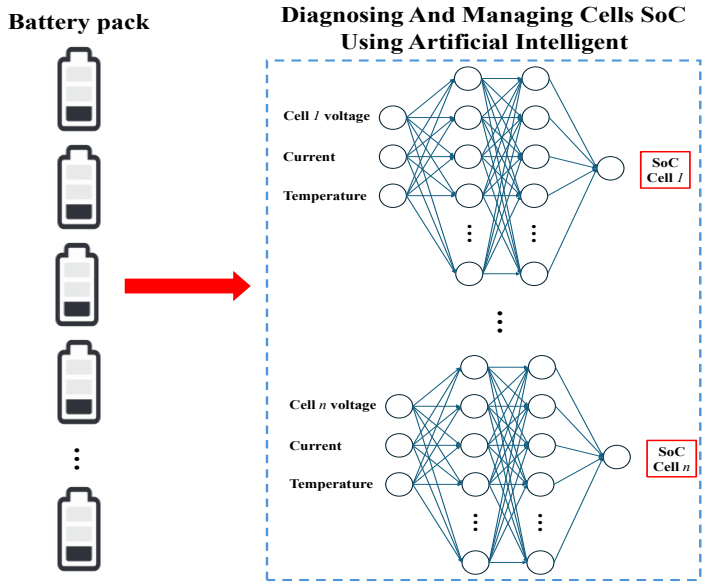

Figure 1. SoC estimation using Artificial Intelligence.

Reference:

[1] N. McIlwaine, A.M. Foley, D.J. Morrow, D. Al Kez, C. Zhang, X. Lu, R.J. Best, A state-of-the-art techno-economic review of distributed and embedded energy storage for energy systems, Energy 229 (2021) 120461. https://doi.org/10.1016/j.energy.2021.120461.

Why Some Soft Ground Settles More than Others: Insights from Subsurface Sedimentary Structure in Deltaic Plains

Anjila Babu Malla[1], Tetsuya Sakai[2] and Toshihide Shibi[2]

[1]Graduate School of Natural Science and Technology, Shimane University, Matsue, Japan
[2]Department of Earth Science, Shimane University, Matsue, Japan

Presenting author: mallaanjila22@gmail.com

Abstract:

Ground settlement and land subsidence are major challenges in low-lying coastal and deltaic regions. Predicting where and why settlements occur remains difficult because subsurface layers with similar thickness or burial depths can behave very differently under loading. The Izumo Plain is an alluvial lowland formed by the infilling of the Paleo-Shinji Bay with sediments supplied mainly by the Hii and Kandogawa Rivers. Thick Holocene mud deposits are widely distributed across the plain, making ground subsidence caused by sediment consolidation a critical geotechnical issue. This study evaluates the subsidence potential of Holocene sediments in the eastern Izumo Plain, with particular emphasis on how sediment type and internal structure jointly influence settlement behavior, particularly in clay-rich deposits.

The study is based on borehole SJ-1 (20.7 m deep), drilled in the eastern part of the Izumo Plain, along the shoreline of Lake Shinji, near the mouth of the Hii River. The borehole core consists sandy to silty sediments down to a depth of 10 m, underlain by thick, soft clayey sediments. Conventional facies descriptions were carried out, and representative undisturbed core sections were selected for laboratory consolidation tests. The clay-rich sediments were further classified based on their internal sedimentary structure into three groups: clay with no structures, clay with faint lamination and clay with well-preserved lamination. These structures reflect how the sediments were deposited originally.

Consolidation tests results show that clay deposits with well-preserved lamination exhibit higher compressibility than with no structures, even at comparable depths. This indicates that internal sedimentary structure, rather than burial depth alone, plays a key role in controlling settlement behavior. Laminated clays tend to preserve an open structure during deposition which collapses readily when loaded, increasing settlement potential.

These findings highlight the importance of identifying clay-rich and structurally weak layers when assessing ground stability. The basic geological and sedimentological information should be incorporated into geotechnical site evaluation, which can improve settlement prediction and support safer infrastructure planning in deltaic plains.

Keywords: Izumo Plain, Ground settlement, Holocene sediments, Clay compressibility.

Holographic Multiplexing in off-axis FMCW-digital holography with Frequency-Modulated and Non-Modulated Light Sources

T. Okamoto[1], I. Okamoto[1], S. Kawabata[1], H. Hamada[1], V. Kumar[1] and M. Yokota[1]
[1]Shimane University
s226010@matsu.shimane-u.ac.jp

In this study, we demonstrate the multiplexing of object wavefronts corresponding to both frequency-modulated (FM) and non-frequency-modulated (non-FM) light sources in the spatiotemporal frequency domain using an off-axis frequency-modulated continuous-wave digital holography (FMCW-DH).

Multimodal (MM) measurement has gained attention in metrology due to advances in analysis techniques that integratively handle multiple observables simultaneously [1]. Digital holography (DH) can discretely record and reconstruct both amplitude and phase of the diffracted light wavefront. We previously proposed an off-axis FMCW-DH by combining the FMCW technique with an off-axis DH configuration [2]. By utilizing both the spatial frequency domain and time frequency domain for multiplexing, the technique can simultaneously record multiple holograms, thereby acquire more information about the target. However, conventional FMCW-DH requires an FM light source, which limits the choice of light sources. In this study, we demonstrate an off-axis FMCW-DH that multiplexes the holograms corresponding to FM and non-FM light sources.

Figure 1 shows the experimental setup. Two laser diodes with center wavelengths of λ_1 = 784.29 nm and λ_2 = 784.866 nm were used as light sources, where LD1 and LD2 are the FM and the non-FM light sources, respectively.

From the time-series holograms recorded by the camera, each wavefront component for two wavelengths can be extracted in the spatiotemporal frequency domain. Subsequently, each wavefront for two wavelengths was numerically reconstructed as shown in Fig. 2. These results demonstrate that the holograms corresponding to both FM and non-FM light sources can be multiplexed in an off-axis FMCW-DH system.

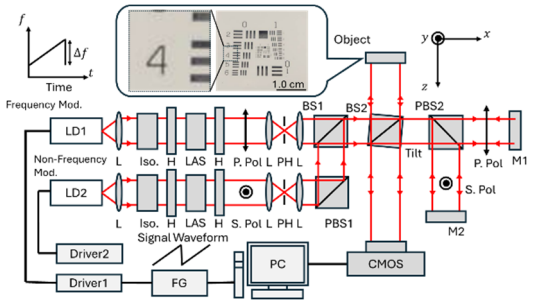

Fig. 2 Experimental setup.

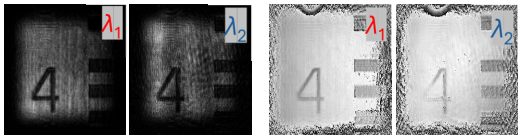

(a) Intensity Image. (b) Phase Image.

Fig. 1 Reconstructed images.

References

[1] Z. M.Zhang et al, The International Journal of Advanced Manufacturing Technology (2023) 124(5),1341–1356, (2023).
[2] H. Hamada et al., Optics Letters. 50(9), 2808-2811, (2025).

Acknowledgement

This work was supported by JSPS KAKENHI Grant Number JP25K07761.

Hilbert transform based four phase-shifting with shadow removal for 3D shape measurement using LCD projector-based fringe projection system

S. Takata[1], V. Kumar[1] and M. Yokota[1]
[1]Graduate School of Science and Technology, Shimane University, Japan
E-mail: s226025@matsu.shimane-u.ac.jp

As a nondestructive and non-contact method for three-dimensional (3D) shape measurement, the liquid crystal display (LCD) fringe projection technique finds its applications in manufacturing, medicine, and cultural heritage preservation. Phase sfifting profilometry (PSP), a notable phase analysis technique in this method increases the number of images to be captured and total acquisition time [1].

This research proposes a method that performs PSP analysis by applying Hilbert transform (HT), which is referred to as HT-PSP. HT outputs the signal with a phase shift of π/2 rad. This method provides four phase shifted fringe patterns from the two projected fringe patterns one with phase 0 rad and other with π rad. This research aimed to implement HT-PSP.

Fig. 1 and shows the experimental setup. *D* is the distance between the projector and camera. *L* is the distance from the reference plane to the camera. In this research, measurement target is stair-shaped object with three steps. To remove shadow areas prior to analysis, a color fringe pattern was used with blue as constant light and red and green as cosine waves.

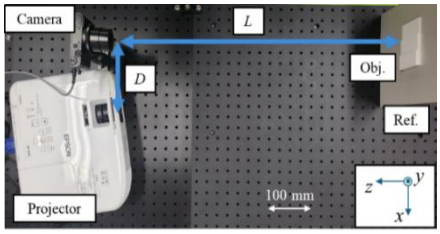

Fig. 1 The experimental setup.

We projected and captured color fringe patterns with initial phases of 0 and π rad. Then, by applying HT to these images, images with initial phases of π/2 and 3π/2 rad were obtained. We performed analysis using the PSP on these four images to obtain the object phase and reference phase. The phase difference between the object and reference plane phase was calculated, and the object shape was then obtained through calibration.

The resulting 3D shape is shown in Fig. 2. We also conducted an FTP analysis and results are shown in Fig. 3.

From Fig. 2 and Fig. 3, the measured results for FTM show more rounded edges compared with HT-PSM results. HT-PSM is better because it performs computation pixel-by-pixel, avoid crosstalk across entire image that occurs in Fourier spectral processing in FTM, also PSM are designed to suppress noise term mathematically making phase extraction less susceptible to random noise and projector nonlinearity.

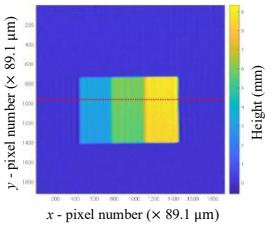

Fig. 2 Measurement result using HT-PSP.

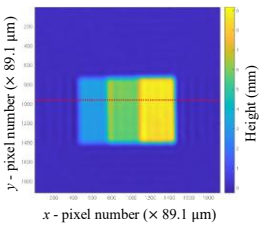

Fig. 3 Measurement result using FTP.

Reference

[1] Varun Kumar : “Liquid Crystal Display Projector Based Fringe Projection System For Three-Dimensional Shape Measurement" M.Tech thesis, Indian institute of technology Delhi, (2010).

Rapid Detection of Mustard Oil Adulteration using an Electronic Nose

Sunitha Mocherla[1], Tatsuyuki Yamamoto[2] and Hemanth Noothalapati[2]

[1]The United Graduate School of Agricultural Sciences, Tottori University, Japan
[2]Faculty of Life and Environmental Sciences, Shimane University, Matsue, Japan

Email: d22a2108@matsu.shimane-u.ac.jp

Introduction: Adulteration of mustard oil with low-cost edible oils is a major challenge in food quality control and authentication. Rapid and reliable screening methods capable of discriminating pure oils and identifying adulteration are therefore required.

Experimental conditions: A Carbon Nanotube (CNT)-based electronic nose (E-nose) was employed to acquire volatile response patterns from pure mustard oil and mustard oil adulterated with canola, cottonseed, palm, rice bran and soybean oils. The sensor responses were evaluated using un-supervised PCA and t-SNE and supervised LR, LDA and SVM machine learning techniques to evaluate discrimination and classification performance.

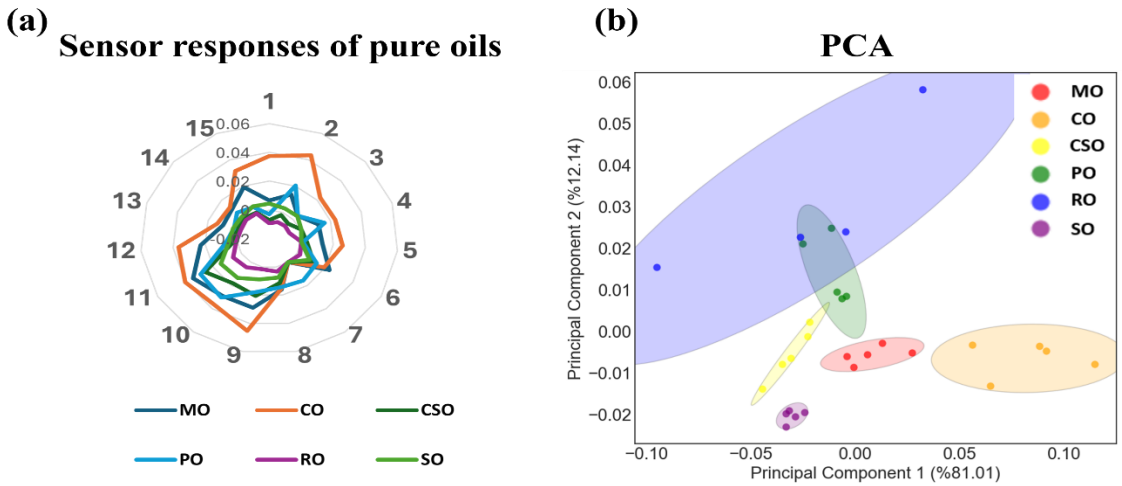

Figure 1.(a) Radar plot showing the Distinct E-nose sensor response patterns of six pure oils. (b) PCA score plot of pure oil samples.

Results and Discussion: Distinct sensor response fingerprints were observed for different pure oils, as illustrated by radar plot of mean E-nose responses (Figure 1a), and PCA revealed clear separation among pure oil types (Figure 1b), demonstrating the inherent discriminatory capability of the E-nose sensor responses. In addition, supervised models successfully classified adulterated mustard oil samples demonstrating the potential of E-nose coupled with machine learning models, as a rapid and reliable tool for mustard oil authentication.

Intelligent Control Methods for High-Efficiency Motor Drive Systems with SiC Inverter used for EVs and Robots

Amy Fedora Felix, Nanditha Dev, Nguyen Gia Minh Thao
[1]Vellore Institute of Technology, India
[2]Shimane University, Japan
amyfedora29@gmail.com, nanditha.dev01@gmail.com, nguyenthao@ecs.shimane-u.ac.jp

Motor drives operating under Field-Oriented Control (FOC) are affected by current harmonics caused by inverter non-linearity and switching effects, leading to increased losses and torque ripple. In three-phase motor drives, the 5th and 7th harmonics are dominant. This work presents a dq-based synchronous reference frame method to extract these harmonic currents under FOC operation. By applying Clarke–Park transformations and harmonic reference frame rotation, individual harmonics are isolated as DC quantities. Simulations are performed at 1500 rpm, and the extracted components are analyzed in the time domain and validated using FFT of steady-state phase currents. A SiC-based inverter modeled in MATLAB/Simulink enables realistic evaluation at high switching frequencies. The proposed approach supports the design of harmonic compensation controllers, such as PI regulators, for mitigating specific current harmonics.

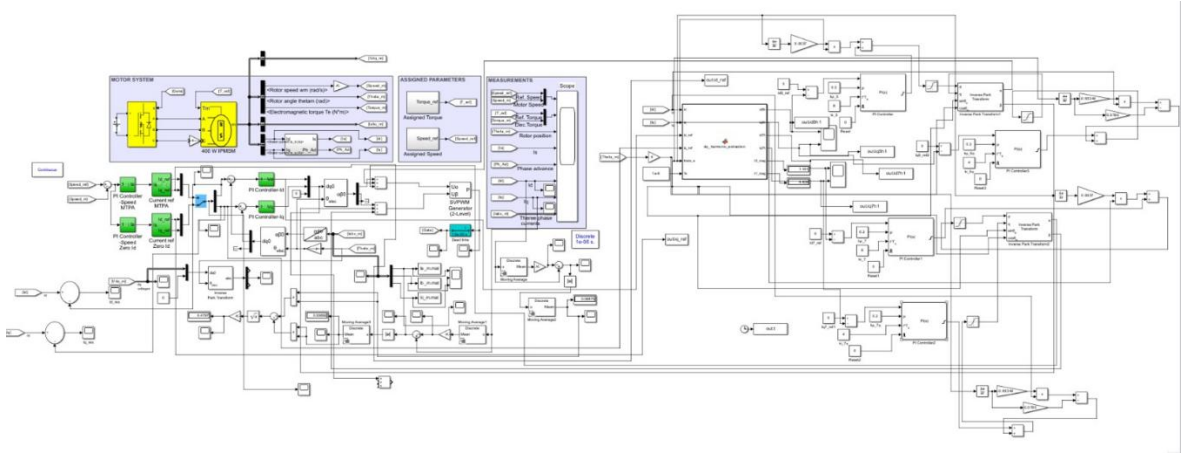

Fig. 1: Simulink Model of IPMSM Motor Drive System

5th Harmonics	
Cut-off Frequency	**Magnitude**
0.5 Hz	0.127
1 Hz	0.1274
2 Hz	0.127
FFT Analysis	0.134772

Table 1: Extracted 5th harmonic magnitude vs. FFT

7th Harmonics	
Cut-off Frequency	**Magnitude**
1 Hz	0.03388
3 Hz	0.03419
5 Hz	0.03616
FFT Analysis	0.0503515

Table 2: Extracted 7th harmonic magnitude vs. FFT

[1] N. G. M. Thao, T. D. Do, D. -K. Ngo and K. Fujisaki, "Novel Auto-Tuning PD-Fuzzy Control of Current Harmonics to Reduce Losses in Motor Drive Systems Excited by SiC-MOSFET Inverter," 2023 SICE International Symposium on Control Systems (SICE ISCS), Kusatsu, Japan, 2023, pp. 103-110, doi: 10.23919/SICEISCS57194.2023.10079198.
[2] Gu, X., Li, Y., Chen, W., & Jin, X. (2022). Improved Deadbeat Predictive Control Based Current Harmonic Suppression Strategy for IPMSM. *Energies*, *15*(11), 3943. https://doi.org/10.3390/en15113943

Valuing Urban Nature: Visitor Preferences and Willingness to Pay for Sustainable Green Space Management: A Case Study of Ramna Park, Dhaka, Bangladesh

Islam Md Rashadul[1] and Tetsuhiko Yoshimura[2]
[1] Graduate School of Natural Science and Technology, Shimane University
[2]Faculty of Life and Environmental Sciences, Shimane University
E-mail: mdrashedjp66@gmail.com

Introduction**:** Dhaka's rapid urbanization has increased pressure on urban parks, while management resources remain limited. This study examines park use, visitor preferences, satisfaction, and willingness to pay for improved park management. Inquiring about WTP makes it easier to gauge how much park visitors value it, assess support for better amenities, and project possible income for sustainable management and understand public attitudes about paying for free-access spaces.

Method: Ramna Park, a significant urban park in Dhaka, Bangladesh. This Park was selected as the study site. Data collected from visitors using a structured questionnaire on September 13,14, and15, 2025, covering park use, preferences, satisfaction, and willingness to pay. Willingness to pay was assessed using the Contingent Valuation Method by asking visitors how much they would pay for hypothetical improvements in park management and services.

Result and Discussion: Of the 292 visitors that took part in the study, 73% were men and 27% were women. Most visitors belonged to the middle-income group (30,001–50,000 BDT), with fewer from low-income and some from higher-income groups. Visitors expressed hopes for better park management by highlighting the need for better park amenities, including restrooms, coffee shops, litter bins, food stores, bookstores, and security cameras. A double-bounded Logit model with CVM was used to estimate WTP. The median entry fee WTP was 28 TK (1 TK = 1.29 Yen) for the full sample (N = 287). After excluding resistance responses, the valid sample decreased to 116, indicating about 60% resistance, and the median WTP increased to 120 TK. About 3,000 people visit Ramna Park daily (PWD). Potential income is roughly 30.7 million TK. per year with a median entry WTP of 28 TK. Although the median WTP increased to 120 TK after excluding resistance responses, this estimate is likely overstated because it does not account for protest responses that reflect widespread opposition to paid entry. Therefore, for a more realistic and policy-relevant assessment, the median WTP of 28 TK derived from the full sample is employed for revenue estimation. The majority of opposition responses were motivated by the belief that park maintenance should be the responsibility of the Dhaka City Corporation and that park entry should remain free to ensure equitable access for all visitors. Many respondents also noted that having to pay an entrance fee on each visit is inconvenient. Although they strongly support improvements in park management and facilities, they believe that such improvements should be funded by the government rather than through user fees.

Market Research and Optimal Pricing of Timber-Based Souvenir Products from the Sanbe Mountain Area

Yue Chen[1] Keisuke Yamanaka[2] and Tetsuhiko Yoshimura[3]
[1]Bioproduction and Bioenvironmental Sciences, Tottori University
[2]University Field Science Center, Faculty of Agriculture, Tottori University
[3]Faculty of Life and Environmental Sciences, Shimane University
E-mail:chebyue3@gmail.com

■ Background

This study aims to identify the price sensitivity and purchasing behavior of young consumers in order to develop souvenir products made from locally sourced timber in the Sanbe Mountain area of Shimane Prefecture. The Sanbe region is rich in natural environments and is strongly associated with forests and grasslands, indicating its high potential as a tourism resource. In the context of increasing demand for sustainable tourism, developing products that utilize unique local resources has become an important issue.

■ Survey Overview

An online questionnaire was conducted using Google Forms on November 13, 2024, targeting 102 students at Shimane University (62 males and 40 females). The purpose of the survey was to examine the market potential of wooden souvenir products.

■ Results

The results revealed that many students had previously visited the Sanbe area and held strong impressions of its natural environment, particularly forests and grasslands. In addition, 97% of respondents stated that they purchase souvenirs when traveling. The main purposes for purchasing souvenirs were “for family and relatives,” followed by “for friends or partners,” and “for themselves.” The most important factors influencing purchase decisions were “regional uniqueness,” “taste of food products,” and “price,” while “product name” and “luxury feel” were less important.

Regarding commonly purchased souvenirs, Western-style sweets were the most frequently chosen both for personal use and as gifts, reaffirming their popularity as travel souvenirs. Wooden products, on the other hand, were often described as “something I would not buy myself but would be happy to receive,” suggesting latent demand. Among wooden items, tableware such as chopsticks, plates, and wooden-handled spoons or forks received the highest preferences, while accessories such as earrings or necklaces showed lower demand, indicating a strong emphasis on practicality.

Furthermore, the PSM (Price Sensitivity Meter) analysis was used to determine the appropriate price ranges for wooden products. The results showed that the acceptable price ranges were 400–512 yen for wooden keychains, 766–1081 yen for wooden cups, and 590–763 yen for wooden earrings. These price ranges reflect levels that young consumers can psychologically accept and provide concrete guidelines for product planning.

■ Conclusion

Overall, souvenir products made from Sanbe-area timber align well with the region’s natural image, and practical wooden tableware in particular has strong potential to stimulate purchasing intentions among young consumers. Setting prices based on PSM analysis can further enhance sales effectiveness. Therefore, this study offers valuable insights for future development of souvenir products utilizing timber from the Sanbe Mountain area.

Space-Resolved Raman Microspectroscopy for Biomolecular Characterization of Colorectal Cancer Cells

Aya Kondo[1], Tatsuyuki Yamamoto[1,2] and Hemanth Noothalapati[1,2]*
[1]Graduate School of Natural Science and Technology, Shimane University, Japan
[2]Faculty of Life and Environmental Sciences, Shimane University, Japan
ayakon0425@icloud.com

Colorectal cancer (CRC) is one of the leading causes of cancer-related mortality worldwide, with more than 1.9 million new cases and approximately 900,000 deaths reported annually. In Japan, around 140,000 new cases are diagnosed each year, resulting in over 50,000 deaths. Improving patient survival strongly depends on early detection and timely initiation of treatment. However, conventional diagnostic methods are often invasive, time-consuming, and susceptible to human error. Therefore, there is a growing demand for non-invasive, rapid, and reliable diagnostic techniques. Raman microspectroscopy, a label-free molecular spectroscopic method, has attracted significant attention due to its ability to provide detailed biomolecular information from living cells. In this study, we aimed to investigate the potential of space-resolved Raman microspectroscopy for biomolecular characterization of colorectal cancer cells. Raman spectra were acquired from colon cancer cells (Caco-2) using a 532 nm excitation laser (NanoFinder 30, Tokyo Instruments). Spectra were collected from four individual cells at five randomly selected intracellular locations per cell, resulting in a total of 20 spectra. The obtained Raman spectra showed variations in characteristic bands associated with protein-rich and lipid-rich components, reflecting intracellular heterogeneity.

Principal component analysis (PCA) was employed to extract dominant spectral features and evaluate variability among cells and measurement locations. The first three principal components explained 97% of the total variance, and the score plots showed distinct distributions depending on individual cells and intracellular regions. These variations are likely attributed to differences in intracellular organelles, membrane composition, or cell cycle stages, even under identical culture conditions.

To establish a robust Raman-based diagnostic method for CRC, it is essential to discriminate cancer cells from normal cells while minimizing intrinsic cellular heterogeneity. Future work will include analyses of multiple colorectal cancer cell lines and normal cells, as well as acquisition of Raman hyperspectral data from a larger number of cells, aiming to develop a rapid, non-invasive, and highly accurate diagnostic platform for colorectal cancer.

A study on the effect of antifungal drug Terbinafine on the metabolism of fission yeast cells by micro-Raman spectroscopy

Tomoki Yamauchi[1], Tatsuyuki Yamamoto[1,2] and Hemanth Noothalapati[1,2*]
[1]Graduate school of Natural Science and Technology, Shimane University, Japan
[2]Faculty of Life and Environmental Sciences, Shimane University, Japan
n25m827@matsu.shimane-u.ac.jp

In recent years, advancements in medical mycology have led to the widespread use of various antifungal agents in clinical practice. Despite this progress, fungal infections such as dermatophytosis and candidiasis remain challenging to treat due to drug resistance and side effects. To mitigate side effects and address the issue of resistant fungi in clinical settings, the development and appropriate utilization of new antifungal agents are essential. Current methods to evaluate new drug candidates require long time and high cost making it difficult for rapid development. Therefore, we need to develop novel techniques that can rapidly evaluate the efficacy of antifungal drugs. This study aims to propose Raman micro-spectroscopy as a viable alternative by demonstrating the inhibition of ergosterol metabolic pathway by antifungal drug Terbinafine in living yeast cells.

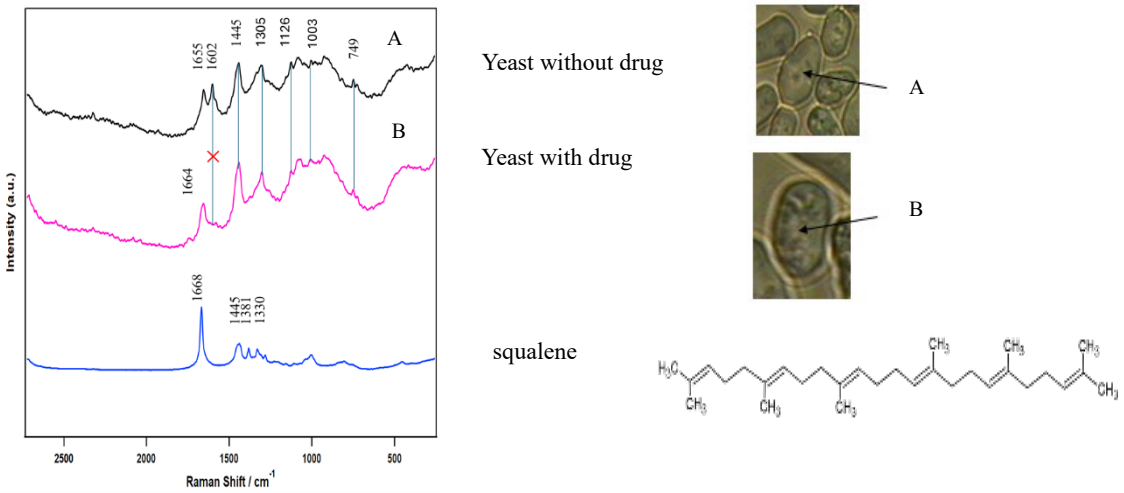

Figure 1. Raman spectra of yeast with and without drug addition (18 hours), and a squalene spectrum. Optical images of yeast cells along with points measured are also shown.

Under 532 nm laser conditions, Raman spectra of yeast cells were measured with and without the drug [Fig 1]. In the absence of the drug, a characteristic Raman band at 1602 cm^{-1}, corresponding to ergosterol in lipid droplets, was clearly observed. This ergosterol marker band remained detectable in lipid droplets even one hour after addition of drug in yeast cells. However, the 1602 cm^{-1} band was no longer detectable 18 hours after addition of drug. Furthermore, the Raman band of squalene in yeast was detected in the absence of ergosterol after 18 hours. Overall, we successfully observed the effect of the antifungal drug Terbinafine on yeast cells using Raman micro-spectroscopy. These findings indicate that Raman spectroscopy has strong potential as a rapid and effective technique for evaluating the efficacy of novel antifungal drugs.

Composition-Dependent Raman and FTIR Spectroscopic Investigation of Solid-State Polyester–Polyurethane Polymer Blends

Suneth Jayasumana[1], Tatsuyuki Yamamoto[2] and, Hemanth Noothalapati[2*]
[1]United Graduate School of Agricultural Sciences, Tottori University-Japan
[2]Faculty of Life and Environmental Sciences, Shimane University-Japan
d24a2108@matsu.shimane-u.ac.jp

Polyester (PES) and polyurethane (PU) powders are widely used in textile-related applications such as heat transfer stickers, coatings, fabric laminations, and as adhesion layers. Blending of PES and PU permits user to adjust properties such as mechanical strength, flexibility, adhesion, and wash durability. However, results often exhibits non-linear property changes may be due to intermolecular interactions. Raman and FTIR spectroscopy offer non-destructive techniques to probe molecular-level changes of PES–PU blends with respect to their compositions.

The objectives of this study to characterize PES and PU powders in pure form and blended forms using Raman and FTIR spectroscopy, in orders to identify composition-dependent spectral trends at micro level in solid state. A set of seven samples of powders were prepared including two pure polymers (100% PES and 100% PU) and five intermediate PES–PU blends. Powders with particle sizes of 80–200 µm were homogenized to ensure uniform blending. By using portable Raman machine with laser excitation of 785 nm spectra were acquired with 5s integration time and averaged over 10 cycles. Ten measurements were collected per sample to assess reproducibility. FTIR measurements were carried out in ATR mode, with each spectrum obtained using 32 scans, and five replicate measurements per sample.

Figure 1 presents the stacked Raman spectra of PES–PU polymer blends across the full composition range from 100% PES to 100% PU. The spectra show consistent changes in ester- and urethane-related bands with changing blend composition, demonstrate a gradual transition from PES-rich to PU-rich chemical features. Further, FTIR also characterized the comparable results to Raman. These results demonstrate that bulk Raman spectroscopy can be used to monitor compositional changes in solid-state PES–PU blends.

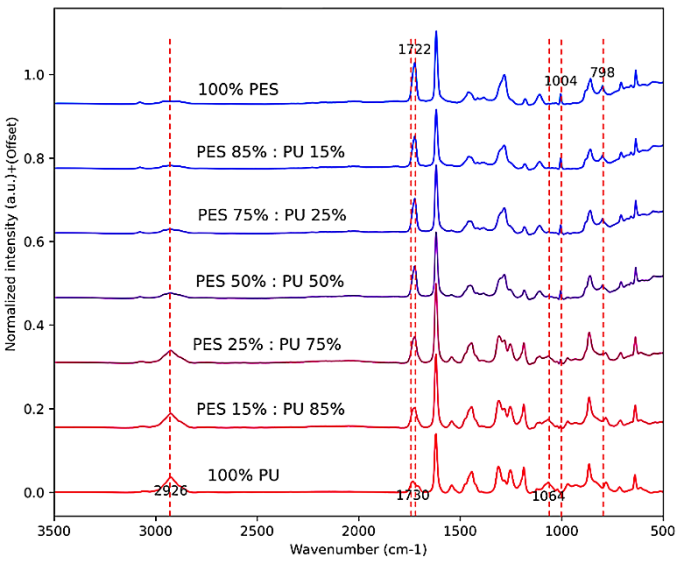

Figure 1. Stacked Raman spectra of PES-PU polymer blends

The future work of this project will require the use of micro-Raman and micro-FTIR analysis in combination with singular value decomposition analysis to determine the heterogeneity of the blends.

Development of a Novel SERS-Based Method for Rapid Detection of Active Pharmaceutical Ingredients at Tracer Levels in Industrial Effluent

Egodage Chavin J Perera[1], Kazuto Arakawa[2], Tatsuyuki Yamamoto[3] and Hemanth Noothalapati[3*]
[1]United Graduate Schools of Agricultural Sciences, Tottori University. Japan.
[2]Next Generation Tatara Co-Creation Centre, Shimane University, 1060 Matsue, Japan.
[3]Faculty of Life and Environmental Sciences, Shimane University, Matsue, Japan.
d24a2107@matsu.shimane-u.ac.jp

Pharmaceutical pollutants, particularly antibiotics and nonsteroidal anti-inflammatory drugs are emerging as serious environmental contaminants, largely due to their improper disposal through industrial effluents worldwide. Their presence in wastewater poses significant risks, including the promotion of antibiotic resistance, endocrine system disruption, and long term ecological toxicity. Conventional detection techniques such as liquid chromatography, although accurate, are often expensive, time consuming, and impractical for rapid or real time monitoring. Raman spectroscopy, a non-destructive and non-invasive analytical technique, offers a promising alternative by providing unique molecular fingerprints of target compounds. However, the detection of trace level pollutants remains a challenge due to inherently weak Raman scattering signals. This project aims to address this limitation by advancing Raman spectroscopy through the integration of Surface-Enhanced Raman Spectroscopy (SERS), with a particular focus on the Shell-Isolated Nanoparticle-Enhanced Raman Spectroscopy (SHINERS) technique. The ultimate objective is to develop a highly sensitive, selective, and efficient platform for the detection of active pharmaceutical ingredients (APIs) at trace concentration levels.

The project adopts a multidisciplinary approach that integrates nanomaterial synthesis, substrate fabrication, and Raman spectroscopic analysis. Figure 1 illustrates the proposed strategy for SERS substrate design: (a) synthesis of gold nanoparticles (AuNPs) with controlled size and shape; (b) coating of ultra-thin silica shells (less than 5 nm) AuNPs to enhance stability and minimize environmental degradation; and (c) rational design of SERS substrates to promote selective molecular interactions with APIs.

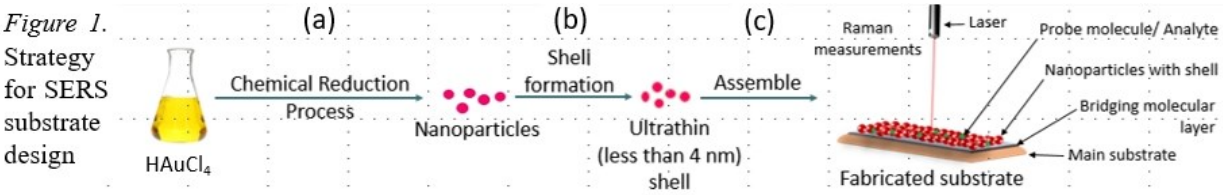

Figure 1. Strategy for SERS substrate design

AuNPs were synthesized using the citrate reduction method, involving the reaction of chloroauric acid with trisodium citrate in an aqueous medium under boiling conditions. The formation of AuNPs was initially confirmed by UV–Vis spectroscopy. Subsequently, silica shell coating was achieved through incubation with a SiO_2 precursor solution for 75 minutes under mild stirring conditions. The morphology of the AuNPs and the successful formation of the silica shell were further characterized using high-resolution transmission electron microscopy (HR-TEM). The SERS performance of the synthesized AuNPs was evaluated using pyridine as a probe molecule and analyzed by micro-Raman spectroscopy. Based on the observed Raman signal enhancement, the SHINERS approach was further investigated using both micro-Raman and portable Raman spectroscopy systems, employing Rhodamine 6G as a model analyte to assess its potential for rapid and on-site detection. Future work will focus on designing SERS substrates to enhance molecular interactions with selected APIs, with particular emphasis on controlling interparticle spacing to maximize signal amplification.